

## Preparation of fine copper powders and their application in BME-MLCC

Songping Wu, Haoli Qin, and Pu Li

College of Chemistry, South China University of Technology, Guangzhou 510641, China

(Received 2005-04-06)

**Abstract:** The preparation of fine copper powders by chemical reduction method was investigated. The reaction of  $[\text{Cu}(\text{NH}_3)_4]^{2+}$  complex with hydrazine hydrate gives spherical monodispersed fine copper powders. The spherical copper powder with a uniform size of  $3.5 \pm 0.5 \mu\text{m}$  was processed to obtain flake copper powder having a uniform size of 8-10  $\mu\text{m}$ , excellent dispersibility and uniform shape. The spherical copper powder of  $2.5 \pm 0.3 \mu\text{m}$  in size, flake copper, glass frit and vehicle were mixed to prepare copper paste, which was fired in 910-920°C to obtain BME-MLCC (base metal multilayer ceramic capacitor) with a dense surface of end termination, high adhesion and qualified electrical behavior. Polarized light photo and SEM were employed to observe the copper end termination of BME-MLCC. The rough interface from the interfacial reaction between glass and chip gives high adhesion.

**Key words:** spherical copper powder; flake copper powder; chemical reduction; BME-MLCC

### 1. Introduction

Thick film technology is widely used for versatile applications [1-2]. Considerable interest for preparing copper end paste has increased during the past few years because of its low cost compared to precious metal paste. Base metal multilayer ceramic capacitor (BME-MLCC) prepared by copper termination paste is seen as a more economical alternative to the conventional precious metal electrode (PME) design. The main reason for this is the replacement of expensive construction materials, such as palladium and silver, with less expensive base metals, namely nickel and copper. BME-MLCC utilize nickel internal electrodes and copper terminations compared to PME-MLCC which use either 100wt% palladium, or the alloy of 30wt% Pd and 70wt% Ag as the electrode material and plateable Ag termination [3].

For conductive paste application, use of high purity crystalline nonagglomerated copper powder that is free from surface oxidation is recommended [4-5]. Precipitation of spherical metallic copper is accomplished through the chemical reduction of a salt, oxide, or hydroxide of copper in solution. Various reducing agents like sodium borohydride [6], starch [7], glycerol [8], *etc.*, have been used for the production of copper powders. Flake copper powders can be prepared using the mechanical method. In conductive paste, the appropriate ratio of spherical and flake copper powders is necessary. The parameters, such as particle size, shape and distribution of metallic powder are of utmost impor-

tance, which have direct bearing on the printing and, in turn, on the microstructure and electrical properties of the resulting films [9-10].

In this paper, a chemical reaction method for the formation of spherical copper particles, and milling process for flake copper powder with a larger particle size and excellent dispersibility are reported. Their applications of BME-MLCC are also studied.

### 2. Experimental

#### 2.1. Preparation of spherical copper powders

All chemicals used were of reagent grade quality, which does not require further purification. Two types of spherical copper powders were prepared with a different feeding order according to the same chemical reaction. In a typical preparation of copper powder, 100 mL solution containing 50 g (80wt%) hydrazine hydrate, 40 g  $\text{CuSO}_4 \cdot 5\text{H}_2\text{O}$ , 15 g  $\text{NH}_4\text{Cl}$  and 70 mL 28wt% aqueous ammonia prepared at room temperature was heated to 80°C for 2 h, to reduce most of the copper ion in the solution to metallic copper. Copper particles designed as Cu-020, which has spherical shape and uniform size in the range of  $2.5 \pm 0.3 \mu\text{m}$ , were formed. Copper powders recovered from the solution were washed and dried under vacuum.

150 mL solution containing 40 g  $\text{CuSO}_4 \cdot 5\text{H}_2\text{O}$ , 4 g sodium tartrate, 15 g  $\text{NH}_4\text{Cl}$  and 70 mL  $\text{NH}_3 \cdot \text{H}_2\text{O}$  was added dropwise for 60 min to a hydrazine hydrate solution under constant stirring. The temperature was kept at 70°C. The solution was heated to 85°C for 1 h to

carry out the reaction sufficiently, to reduce most of the copper ion in the solution to metallic copper having spherical-like shape and uniform size in the range of  $3.5 \pm 0.5 \mu\text{m}$ , which was designed as Cu-040.

## 2.2. Preparation of flake copper powders

50 g above-mentioned Cu-040 spherical copper powders, 900 g  $\text{ZrO}_2$  milling media and dispersing agent were mixed in a vessel. The sealed vessel was fixed in planet-type grinding mill and rotated 10 h to obtain flake copper powders having average congeries sizes ( $D_{50}$ ) of 8.0-10  $\mu\text{m}$ . The flake copper powders were recovered from the solution, washed and dried under vacuum.

## 2.3. Preparation of termination of BME-MLCC

Appropriate resin, which should burn out easily and cleanly under nitrogen, ratio of spherical copper and flake and glass, which is stable under high firing temperature and a nitrogen atmosphere, acid resistance and good wettability to the selected copper powder, were chosen to prepare thick film paste containing 60wt%-70wt% copper. The paste was rolled several times using a three-roll mill and was coated on the green chip, and then was subjected to drying for 15 min at  $120^\circ\text{C}$  to remove the major portion of the volatile organic solvent. Copper end terminations were fired at suitable temperature for 10 min in a nitrogen atmosphere, with a controlled level of oxygen, to obtain BME-MLCC.

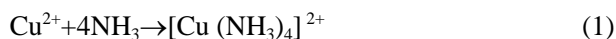
Direct observation of the powder was made by scanning electron microscopy (SEM) on a XL30 $\delta$  DX-4I (Phlip) to reveal the shape of the particles, their diameter and size distribution. The mean sizes and the stand deviations were estimated from image analysis using a laser size distribution analyzer (LS230). The crystal structure was characterized by X-ray diffraction. The purity of powder was determined with ICP (PE Optima 3000). The BME-MLCC were fixed with resin and processed using a grinding and polishing machine. The connection of internal-terminal electrode and the distribution of glass and copper in termination were observed by polarized light microscope (Olympus BX51M). The capacity (Cap), dissipation factor (DF) and insulation resistance (IR) of BME-MLCC were determined by HP4278A electric meter (USA) and SF2512 insulation resistance apparatus (China), respectively. The adhesion strength of electrode was determined with FDV-50 force apparatus (Wagner Instruments, USA).

## 3. Results and discussion

### 3.1. Basic chemical reaction and preparation of copper powders

In this experiment, hydrazine hydrate and

$\text{NH}_4\text{Cl}/\text{NH}_3\cdot\text{H}_2\text{O}$  were chosen as reductant and buffer agent, respectively. The solution was blue before being reduced, and became yellow afterward. In this process, the following chemical reaction occurred:



In aqueous ammonia media, ammonia reacts with  $\text{Cu}^{2+}$  according to Eq. (1) and  $[\text{Cu}(\text{NH}_3)_4]^{2+}$  complex was reduced to obtain fine copper powder as Eq. (2).

For preparing fine powder by chemical reduction method, it is very important to choose appropriate dispersion agent. Generally speaking, dispersion agent absorbs on the solid-liquid interface and forms a layer of molecular membrane to hinder inter-contact between the particles and at the same time, it reduces surface tension, thereby reducing the absorption capability of the capillary. It can be distinctly observed that the micron-sized monodispersed and nonagglomerated particles of copper were prepared when inorganic dispersing agent, namely sodium tartrate, was employed. The results are showed in Fig. 1. The formation of "monodispersed" particles proceeds through a two-stage mechanism, the primary particles are produced first, and then aggregate to larger final products. There are two possible mechanisms involved in the aggregation based on either diffusion-limited or reaction-limited processes. The subunits have to overcome an energy barrier to effectively collide with growing particles. If the driving force is high enough, aggregation is rapid and the rate is limited by the diffusional motion of the colliding subunits. The highly concentrated small crystallites aggregate to large spherical particles owing to their faster Brownian motion and higher collision efficiency.

In the course of reaction of Cu-040, addition of dispersed  $\text{CuSO}_4$  droplet to the dispersed hydrazine hydrate is important which shows that a confined amount of copper ion in a droplet of  $\text{CuSO}_4$  may govern the size of the particles in copper powders as seen in Fig. 1(b). In the absence of dispersion agent, it is possible that monodispersed particles tend to grow once copper ion remains in the solution. The purity of copper powder was analyzed with ICP. The results showed that its purity was more than 99.9wt%.

Fig. 2 shows the XRD pattern of the product prepared by the solution containing  $[\text{Cu}(\text{NH}_3)_4]^{2+}$  complex and hydrazine hydrate. From the pattern, it is obvious that the diffraction graph exhibits the characteristic peaks of crystalline metallic copper (fcc).  $d = 2.0895, 1.8089, 1.2792$  respectively, which is very close to that given by JCPDS file no.4-836 ( $d = 2.088, 1.808, 1.278$ ).

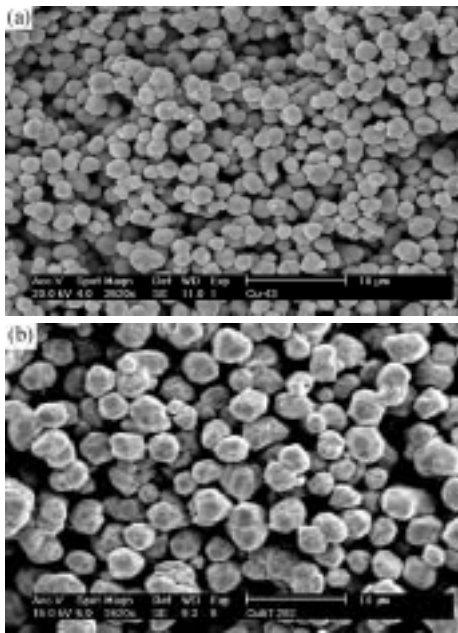


Fig. 1. SEM photographs of ultrafine powders prepared by different feeding orders: (a) Cu-020; (b) Cu-040.

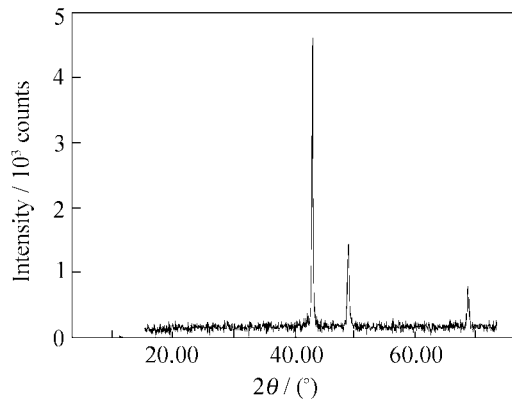


Fig. 2. XRD spectrum of copper powders.

The flake copper powder was prepared by planet grinding mill using the Cu-040 as the precursor spherical copper powders. The SEM photograph and size distribution pattern of flake copper powder are given in Fig. 3. In Fig. 3, monodispersed nonagglomerated flake copper powder was prepared after 10 h mill. The size of circular flake copper particles having controllable ratio of diameter to thickness and surface area (about 0.4-0.8 m<sup>2</sup>/g) is even. The normal and narrow size distribution of powders indicates the excellent dispersibility of powders. The excellent dispersibility of flake coppers is attributed to the good dispersibility of precursor spherical copper powders and the powerful dispersion effect produced by milling.

### 3.2. Preparation of copper termination paste

The copper termination paste consists primarily of three functional constituents: (1) the metal powder with excellent dispersibility, namely above-mentioned 35wt% spherical Cu-020 and 33wt% flake coppers, which provide the conductive phase; (2) glasses or

oxides, namely B<sub>2</sub>O<sub>3</sub>-SiO<sub>2</sub>-ZnO glass frit and ZnO, which act as a permanent binder and also promote sintering of metal powders during firing and enable binding of the termination to the chip, and the glass frit added to the paste was smelted at 1350°C and fritted to an average particle size of 3-4 μm; (3) organic phases, which disperse the metal and binder component to impart the desired rheological properties to the paste.

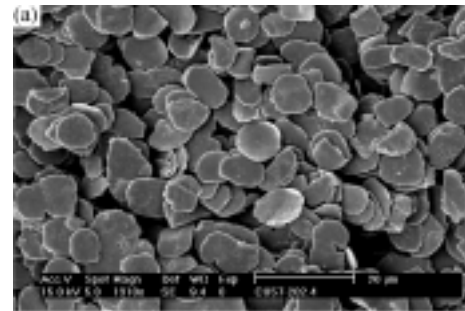


Fig. 3. SEM photograph (a) and size distribution pattern (b) of flake copper powders.

The rheological behavior is primarily controlled by the nature of powder, dispersion process and vehicle. Insufficient wetting of compacted agglomerate particles leads to formation of copper flocks in the paste, which is undesirable for thick film applications. However, effective wetting of monodispersed nonagglomerated powders results in the formation of a stable paste with a high degree of dispersion, which is desirable for thick film application. Three-roll mill is an effective equipment to destroy soft agglomeration of powders in paste owing to its great mechanical power. The organic vehicle plays an important role in wetting the powder surface. The vehicle is a temporary ingredient blend of some solvents and polymers or resins to provide a homogeneous suspension of the particles of the functional materials and a rheology suitable for the making termination of BME-MLCC.

### 3.3. Densification of termination and diffusion of metal on glass bubbles

The copper end termination of BME-MLCC was processed through paste-making, coating termination, drying and firing. The decomposition of vehicle organics and crystallization of copper powders occur in the process of firing. The densification of end termina-

tion of BME-MLCC and the state of glass have great effect on electroplating, solderability and solder leaching resistance. The microstructures of end termination prepared at different firing temperatures are given in Fig. 4, which shows lots of glass bubbles on the end face of BME-MLCC when the firing temperature is 845°C, and the film fired shows vertical grain growth. Bad wetting behavior of glass frit to chip results in the loose end face, which is unfavorable for electroplating and solderability. However, when the firing temperature is 910°C, excellent densification appears, and the grain growth is lateral. Dense film can prevent electroplating solution from penetration, avoid failure and is favorable for solderability. It shows that the wetting behavior of glass frit to chip is considerably

dependent on the temperature. The wetting behavior of glass increases with increasing firing temperature. It was reported [11] that the densification of the film depends on the contact area and the glass particle size distribution before and after softening of the glass, respectively. The effect of glass addition on the densification is more obvious with small size silver particles. This can be interpreted in terms of silver–glass interaction, good sinterability of silver and large silver–glass area obtainable with fine silver powder [12]. In this work, since the powders including copper powders and glass frit have small size and excellent dispersibility, dense copper end termination can be prepared at suitable firing temperature.

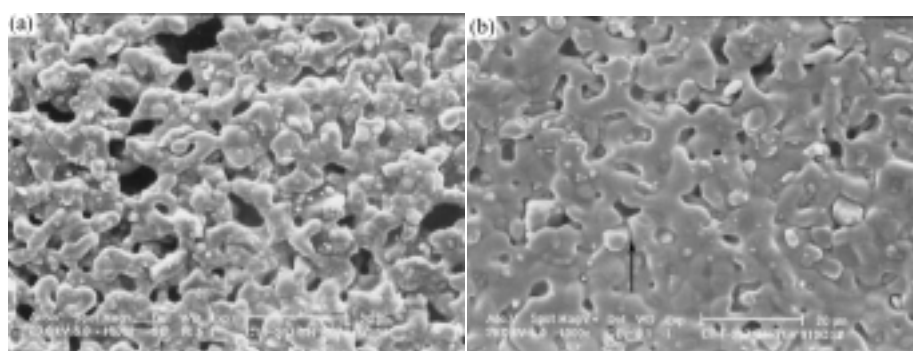


Fig. 4. SEM photographs of end termination of electrode at different firing temperatures: (a) 845°C; (b) 910°C.

A glass bubble with a diameter of 5  $\mu\text{m}$ , which is shown in Fig. 4(b), was selected to study the diffusion of copper on the surface of the bubble. As shown in Fig. 5, the contents of copper are 65wt%, 72wt% at the core and interface of the bubble, respectively. The content of copper is up to 90% at outside the interface. It shows that the mutual diffusions between copper and glass appear in the firing process. Generally speaking, the higher content of metallic copper of small size glass bubbles indicates better electroplating behavior and better solderability, and the lower content of metallic copper of large size glass bubbles shows poor electroplating behavior and poor solderability. It is in good accordance with experimental results.

### 3.4. Connection of internal-terminal electrode

The SEM photograph of the fired termination of BME-MLCC corresponding to 10wt% glass is shown in Fig. 4(b). The glass frit is composed of  $\text{B}_2\text{O}_3\text{-SiO}_2\text{-ZnO}$  glass and ZnO with a ratio of 6:4. Zinc oxide plays an important role in this glass system. Adhesion strength and solderability of a copper thick film on an alumina substrate were studied by Toshio Ogawa *et al.* [13]. The films with an addition of glass frit or mixtures of glass frit and metal oxide do not provide good adhesion and solderability simultaneously. However, the copper thick film containing 10wt% bismuth oxide has

excellent characteristics, *i.e.* high adhesion strength, good solderability, and low sheet resistivity. In this experiment, zinc oxide was employed to obtain good copper end termination with excellent characteristics.

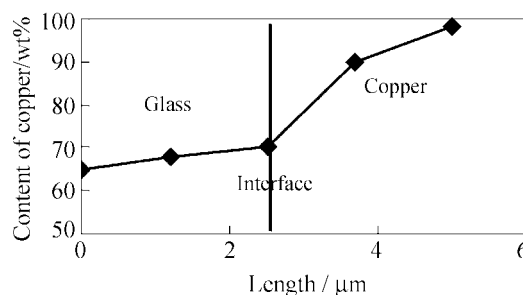


Fig. 5. Diffusion of copper to glass.

The electrical behavior and reliability of BME-MLCC are greatly affected by the connection of internal-terminal electrodes and termination to chip. The connection of termination to chip is attributed to the interface reaction between glass and chip. The SEM photographs of section of BME-MLCC fired at the peak firing temperature from 845 to 935°C adopting the same firing cycle are shown in Fig. 6. The interface states obtained at different firing temperatures are different. The changes of interface states with temperature can be well explained by the wetting and interfacial reaction. Since the wetting behavior of glass frit to

chip is considerably dependent on the temperature [13], the properties of the copper end termination will be correspondingly affected by the sintering temperature.

Effective connection between copper termination and chip does not appear due to the large wetting angle of glass frit at the peak firing temperature of 845°C as

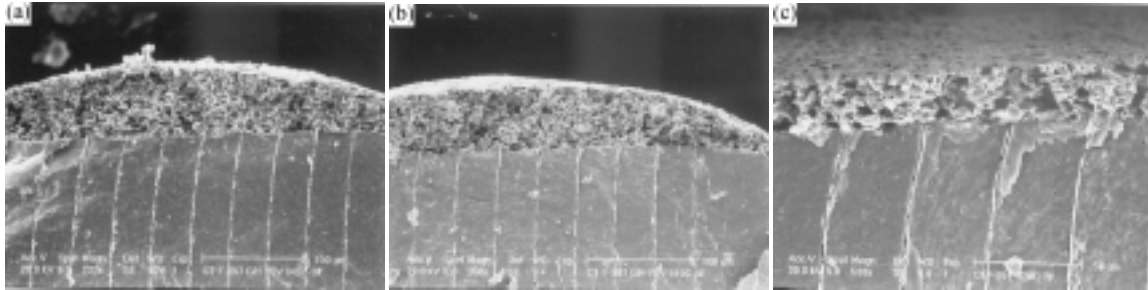


Fig. 6. SEM photographs of section of BME-MLCC at different firing temperatures: (a) 845°C; (2) 910°C; (3) 920°C.

Rough interface between termination and chip occurs at the peak firing temperatures of 910-920°C in Fig. 6(b), and its adhesion strength is up to an average of 3.55 kg owing to small wetting angle of glass frit, which could be attributed to interfacial reaction. However, with the subsequent increase in temperature to 940°C, the adhesion strength decreases. It might be due to the appearance of microcracks in the chip because of too strong interfacial reaction at the higher firing temperature.

The glass spread on copper develops good adhesion strength. The driving force for spreading is provided by the reduction of interfacial energy caused by the reaction between chip and glass. Wetting and interface reactions in lead borosilicate glass-precious metal systems have been studied by Nagesh *et al.* [14]. They reported that increasing wetting or decreasing contact angle could be attributed to interfacial reactions. A sharing of oxygen with a continuity of electronic structure across the interface (chemical bonding) causes a reduction in the interfacial energy and strong adhesion. Bonding behavior of copper thick films containing lead-free glass frit on aluminum nitride substrates was studied by X.R. Xu *et al.* [9]. They reported that the reaction between glass and substrate gives high adhesion strength, which is in agreement with the observations made during this experiment, *i.e.*, rough, porous microstructure in the copper/glass-chip interface increases the adhesion strength. Thus, the copper/glass-chip rough interface plays an important role in the adhesion strength of the BME-MLCC.

### 3.5. Polarized light microscope study

The BME-MLCC prepared at the peak firing temperature of 920°C was processed with a polishing machine. The polarized light microscope photo of section of polished BME-MLCC is shown in Fig. 7. From this

photo, the connection of internal-terminal electrode is very obvious, and the distribution of glass in termination is even. A gray bond occurs between termination and chip. The gray bond can be reasonably explained as the result of interface reaction. To avoid the interfacial cracks that are believed to result from the thermal expansion mismatch between reaction bond and chip, a suitable firing temperature was employed. Therefore the reaction bond in this work is very thin (about 2 μm), implying the low residual tension stress between reaction bond and chip, which was demonstrated to increase with the thickness of the reaction layer [12].

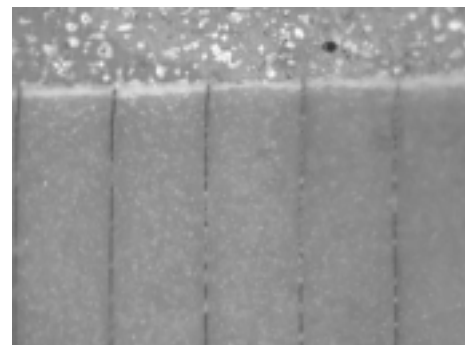


Fig. 7. Polarized light photo of section of MLCC.

### 3.6. Behavior of BME-MLCC

The electrical-physical behavior of BME-MLCC is listed in Table 1. The capacity, DF and insulation resistance of BME-MLCC are qualified. The average adhesion strength of electrode is 3.55 kg. The coverage rate of new solder on the top face of terminal electrode is 95%. The solderability behavior of MLCC was tested for 5 s at  $235 \pm 5^\circ\text{C}$  and the result demonstrated excellent solderability. The resistance behavior to soldering was tested for 5 s at  $260 \pm 5^\circ\text{C}$ , and the coverage rate of new solder on terminal electrode was 95%.

Table 1. Behavior of BME-MLCC

Cap / nF	DF / 10 <sup>-4</sup>	IR / $\Omega$	Solderability	Solder leaching resistance	Adhesion strength / kg
103-107	58-69	> 5 $\times$ 10 <sup>9</sup>	> 95%	> 95%	3.55

#### 4. Conclusions

The spherical copper powders by chemical reduction method were synthesized. Copper particles of spherical shape and uniform size in the range from  $2.5 \pm 0.3 \mu\text{m}$  to  $3.5 \pm 0.5 \mu\text{m}$  were formed when different processes were employed. These larger particles were processed using a planet grinding mill to obtain flake copper with an average congeries sizes ( $D_{50}$ ) of 8.0-10  $\mu\text{m}$ . The former spherical copper powder, flake copper, glass frit and vehicle were mixed to prepare copper paste. The copper paste was coated on the termination of chip, and then fired at a suitable temperature of 910-920°C. The BME-MLCC with a dense surface of end termination, high adhesion and qualified electrical behavior were prepared. The rough interface from the interfacial reaction between glass and chip gives high adhesion.

#### References

- [1] S. Rane and V. Puri, Thick film dielectric overlay effects on thin and thick film microstrip bandpass filter, *Microelectronics*, 32(2001), No.8, p.649.
- [2] B. Su and T.W. Button, The processing and properties of barium strontium titanate thick films for use in frequency agile microwave circuit applications, *J. Eur. Ceram. Soc.*, 21(2001), p.2641.
- [3] T. Addona, P. Auger, C. Celik, et al., Nickel and copper powders for high capacitance MLCC manufacture, *Passive Compon. Ind.*, 11(1999), p.14.
- [4] R. Sarraf-Mamoory, G.P. Demopoulos, and R.A.L. Drew, preparation of fine copper powders from organic media by reaction with hydrogen under pressure: Part II. The kinetics of particle nucleation, growth, and dispersion, *Metall. Mater. Trans. B*, 27(1996), No.4, p. 577.
- [5] B. Langner, A. May, R.H. Wilde, *Process for Producing Nonferrous Metal Powder*, US Patent 4818280, USA, 1989.
- [6] A. Sinha, S.K. Das, T.V. Kumar, et al., Synthesis of nano-sized copper powder by an aqueous route, *J. Mater. Synth. Process.*, 7(1999), No.6, p.373.
- [7] Tani, Hiroji, Ogata, et al., *Production of Copper Powder*, US Patent 5850047, USA, 1998.
- [8] A. Sinha and B.P. Sharma, Preparation of copper powder by glycerol process, *Mater. Res. Bull.*, 37(2002), p.407.
- [9] X.R. Xu, H.R. Zhuang, W.H. Li, et al., Bonding behavior of copper thick films containing lead-free glass frit on aluminum nitride substrates, *Ceram. Int.*, 30(2004), p.661.
- [10] S.B. Rane, P.K. Khanna, T. Seth, et al., Firing and processing effects on microstructure of fired silver thick film electrode materials for solar cells, *Mater. Chem. Phys.*, 82(2003), p.237.
- [11] K.I. Yajima and T. Yamaguchi, Sintering and microstructure development of glass-bonded silver thick films, *J. Mater. Sci.*, 19(1984), p.777.
- [12] S.B. Rane, T. Seth, G.J. Phatak, et al., Influence of surfactants on silver powder and its thick films, *Mater. Lett.*, 57(2003), p.3096.
- [13] T. Ogawa, M. Otani, T. Asai, et al., Effect of inorganic binders on the properties of thick film copper conductor, *IEEE Trans. Compon. Packag. Manuf. Technol. Part A*, 17(1994), No.4, p.625.
- [14] V.K. Nagesh, A.P. Tomsia, and J.A. Pask, Wetting and reactions in the lead borosilicate glass-precious metal systems, *J. Mater. Sci.*, 18(1983), p.2173.